

# Dependency Structure Augmented Contextual Scoping Framework for Multimodal Aspect-Based Sentiment Analysis

Hao Liu  
Xi'an Jiaotong University  
Xi'an, China  
haoliu88@stu.xjtu.edu.cn

Lijun He  
Xi'an Jiaotong University  
Xi'an, China  
lijunhe@mail.xjtu.edu.cn

Jiaxi Liang  
Xi'an Jiaotong University  
Xi'an, China  
liangjiaxi@stu.xjtu.edu.cn

Zhihan Ren  
Xi'an Jiaotong University  
Xi'an, China  
renzh@stu.xjtu.edu.cn

Fan Li  
Xi'an Jiaotong University  
Xi'an, China  
lifan@mail.xjtu.edu.cn

## ABSTRACT

Multimodal Aspect-Based Sentiment Analysis (MABSA) seeks to extract fine-grained information from image-text pairs to identify aspect terms and determine their sentiment polarity. However, existing approaches often fall short in simultaneously addressing three core challenges: Sentiment Cue Perception (SCP), Multimodal Information Misalignment (MIM), and Semantic Noise Elimination (SNE). To overcome these limitations, we propose DASCO (Dependency Structure Augmented Scoping Framework), a fine-grained scope-oriented framework that enhances aspect-level sentiment reasoning by leveraging dependency parsing trees. First, we designed a multi-task pretraining strategy for MABSA on our base model, combining aspect-oriented enhancement, image-text matching, and aspect-level sentiment-sensitive cognition. This improved the model's perception of aspect terms and sentiment cues while achieving effective image-text alignment, addressing key challenges like SCP and MIM. Furthermore, we incorporate dependency trees as syntactic branch combining with semantic branch, guiding the model to selectively attend to critical contextual elements within a target-specific scope while effectively filtering out irrelevant noise for addressing SNE problem. Extensive experiments on two benchmark datasets across three subtasks demonstrate that DASCO achieves state-of-the-art performance in MABSA, with notable gains in JMASA (+3.1% F1 and +5.4% precision on Twitter2015).

## CCS CONCEPTS

• Information systems → Sentiment analysis; Information extraction; Multimedia and multimodal retrieval.

## KEYWORDS

Multimodal Aspect-Based Sentiment Analysis, Dependency trees, Scope

## 1 INTRODUCTION

Multimodal Aspect-Based Sentiment Analysis (MABSA) [13, 18, 27, 46] is a cutting-edge research direction in affective computing, focusing on extracting fine-grained associative semantic and sentiment information from heterogeneous modal data (text-image pairs). Unlike traditional unimodal sentiment analysis approaches, which relies solely on textual data, MABSA leverages cross-modal feature alignment to enhance the identification of aspect terms and

their sentiment orientations. The MABSA framework encompasses three key subtasks: Multimodal Aspect Term Extraction (MATE), Multimodal Aspect Sentiment Classification (MASC), and Joint Multimodal Aspect Sentiment Analysis (JMASA). Specially, MATE [11, 16, 17] concentrates on identifying all aspect terms in sentences; MASC [7, 41] aims to determine the sentiment polarity (positive, negative, or neutral) for each identified aspect term; and JMASA [13, 18, 46] jointly models aspect-sentiment pairs in an end-to-end fashion.

Existing research on MABSA [13, 19, 21, 23, 25, 35, 36, 38, 40, 47] mostly relies on using pre-trained models (such as BERT, RoBERTa, ResNet, CLIP [5, 6, 22, 29]) to extract visual and textual features. These pre-trained models usually use general vision-language understanding tasks such as next sentence prediction (NSP), masked language modeling (MLM), image classification, and image-text matching (ITM) as their pre-training objectives. However, there are significant differences between these pre-training objectives and the task objectives of MABSA [18], resulting in serious misalignment issues when models attempt to capture fine-grained aspects, opinions, and sentiment cues in language and visual modalities, and making it difficult to ensure consistency across modal information. We summarize this type of challenge as the *Sentiment Cue Perception (SCP)* challenge.

Furthermore, the inherent heterogeneity of image-text data naturally leads to information asymmetry and mismatch issues, which further increases the difficulty of multimodal feature alignment and fusion. As shown in Figure 1.A, the "Digital logic" content displayed in the image is not mentioned in the text, while the "circuit problem" mentioned in the text is difficult to strictly correspond with only the circuit structure and basic knowledge presented in the image. Additionally, descriptions such as "clever," "quickly," and "sophisticated" in the text cannot be directly obtained from the image; similarly, although the text description of "student" is full of positive sentiment, this sentiment cue is difficult to explicitly capture in the image. We summarize this phenomenon as the *Multimodal Information Misalignment (MIM)* challenge.

To address the MIM problem, existing research [13, 19, 21, 38] has proposed various methods, such as text-driven image representation alignment and cross-modal relationship detector construction. These methods mainly rely on attention mechanisms for semantic association modeling, but when the input text contains multiple aspects, the inherent noise propagation characteristics of attention

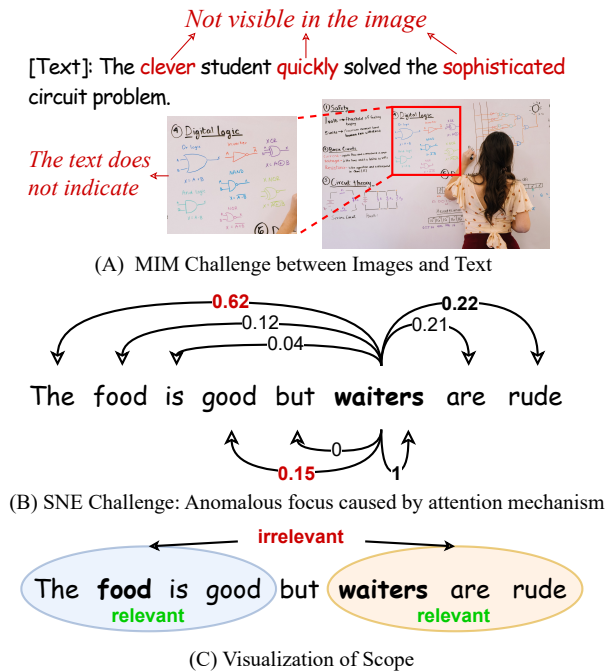


**Figure 1: Partial challenges in MABSA and Visualization of Scope.**

mechanisms may weaken key semantic cues. As shown in Figure 1.B, when analyzing a sentence with contrasting sentiments "The food is good but waiters are rude," the BERT model [5] exhibits clearly irrational attention distribution for the word "waiters": although this word receives the highest attention weight to itself (1.0), its attention to the core sentiment word "rude" (0.22) is significantly lower than to the initial definite article "The" (0.62), and it even maintains abnormal attention to the positive sentiment word "good" (0.15). This counter-intuitive attention distribution pattern is attributed to noise interference in the attention mechanism, which we systematically define as the *Semantic Noise Elimination (SNE)* challenge.

To tackle the challenges mentioned above, we propose a Dependency Structure Augmented Contextual Scoping Framework (DASCO). The DASCO framework consists of two phases: in the first phase, we design aspect-oriented enhancement (AOE) and aspect-level sentiment-sensitive cognition (ASSC) pre-training tasks for the base models (Qformer [15] and language model). Compared to traditional pre-training methods, our training objectives focus more specifically on aspects and sentiments, tailored for the MABSA task. During the joint pre-training of image and text modalities, our approach effectively attends to and integrates aspect and sentiment information from each modality, thereby effectively alleviating the SCP challenge. Additionally, we constructed an image Scene Graph dataset using GPT-4o [26]. Scene Graphs provide structural descriptions of each image, clearly articulating visually apparent content through text, efficiently supplementing textual information. The Scene Graph is input into the Qformer alongside the image,

enabling mapping of image features to the textual domain and accomplishing feature bridging and alignment between images and text. Simultaneously, we retain the traditional image-text matching (ITM) pre-training task from conventional MABSA designs [18, 27]. Both the Scene Graph design and the ITM task together effectively mitigate the MIM problem.

In the second phase, we introduce dependency relations as a syntactic branch alongside the traditional semantic branch. Dependency relationships [2, 4, 24, 31] have demonstrated significant effectiveness in text-only ABSA task by helping models identify other lexical items that are most closely related to a specific word. However, the application of dependency relations in MABSA tasks has not received sufficient attention. The DASCO framework explicitly incorporates the entire dependency structure as input to the model, enabling it to fully utilize global syntactic information. Concurrently, we leverage dependency trees to define semantically relevant contextual boundaries (scopes) for target words, as illustrated in Figure 1.C. During the final classification process, the model focuses exclusively on effective semantic features within the defined scope, thereby reducing potential semantic noise that may arise from sole reliance on attention mechanisms, thus alleviating the SNE problem.

In summary, our contributions are as follows:

- We propose DASCO, a two-phase framework addressing MABSA challenges through base model pretraining and dependency structure augmented contextual scoping, achieving state-of-the-art performance across three subtasks.
- To address the misalignment between traditional vision-language pretraining tasks and MABSA, we introduce aspect oriented enhancement and aspect-level sentiment-sensitive cognition pretraining tasks tailored for MABSA, enabling the extraction of aspect-specific and sentiment-sensitive features to effectively address the SCP challenge.
- We construct an image Scene Graph dataset presenting structured visual information in textual form which, combined with image-text matching pretraining task, effectively mitigates the MIM problem.
- To address the SNE challenge, we integrate dependency structure into a syntax-semantic dual branch architecture with contextual scoping that reduces irrelevant noise, enabling precise aspect and sentiment discrimination.

## 2 RELATED WORK

**Multimodal Aspect-based Sentiment Analysis** MABSA is a prominent research direction in affective computing. Its core challenge lies in accurately perceiving and modeling aspect information and multimodal sentiment cues. Based on the issues addressed by existing methods, mainstream MABSA approaches can be broadly categorized into two types:

*The first type focuses on Multimodal Information Misalignment (MIM).* JML [13] and CORSA [21] both introduce additional relation detection modules to extract text-relevant image features, alleviating inconsistencies between objects referenced in images and text. JCC [19] and CMMT [38] construct text-guided cross-modal fusion modules that dynamically model the contribution of multimodal features to each aspect. Atlantis [36] enhances cross-modal

information integration through image aesthetic evaluation and multi-granularity fusion strategies. AESAL [47] combines aspect-enhanced pre-training task with syntactic adaptation to more thoroughly capture visual-aspect associations and word importance. VLP [18] designs pre-training objectives for language, vision, and cross-modal task-specific targets, effectively improving fine-grained modeling and alignment.

*The second type targets eliminating semantic noise (SNE).* M2DF [44] leverages curriculum learning to reorder training samples, mitigating noisy image interference without explicit data filtering, and improving robustness. AoM [46] introduces aspect-aware attention mechanisms and explicit sentiment embeddings to highlight aspect-relevant content and suppress irrelevant noise. DQPSA [27] uses a dual-query prompting mechanism to strengthen the link between visual features and analytical targets. RNG [23] integrates global correlation, information bottleneck, and semantic consistency constraints to address multi-level noise and multi-granularity semantic gaps in multimodal features.

Despite notable advances, existing methods still remains limitations: some rely too heavily on feature extractors [8, 13, 19–21, 23, 30, 38, 47], others are entirely attention-based [13, 19, 36, 38], and many focus exclusively on MIM [18] or SNE [27, 44, 46]. As a result, **they still fall short in jointly addressing the triple challenges of SCP, MIM, and SNE.**

**Dependency Trees in MABSA** Dependency Trees have been widely applied in text-only ABSA [2, 4, 24, 31], proving effective in capturing syntactic structures. However, their application in MABSA remains relatively underexplored. AoM [46] constructs a Boolean dependency matrix where entries are set to 1 for word pairs with parent-child relationships. This matrix is then used to weight correlations between atomic features, enabling each atomic feature to focus on its most relevant parts. Although this method alleviates semantic noise, the dependency information is only implicitly injected via hard weighting without being directly input to the model. Moreover, limiting the structure to parent-child nodes is overly rigid and may overlooking other valuable syntactic cues. Similarly, AESAL [47] incorporates dependency relations by constructing weighted matrices based on first-order, second-order, and global dependency nodes. Weights are assigned using dependency distances computed via breadth-first search. While such method can mitigate noise, they rely on static, rule-based weighting mechanisms that lack the capacity to capture the dynamic and nuanced syntactic relationships encoded in dependency trees, resulting in numerous potential syntactic patterns remaining unrecognized by the model.

In summary, existing methods largely treat dependency information as an auxiliary weighting tool, limiting its effectiveness in syntactic modeling. In contrast, DASCO explicitly feeds complete dependency structures into the model, enabling it to perceive global syntactic dependencies. We further integrate a Scope mechanism to constrain effective semantic range, which effectively avoids information loss problems caused by hard weighting while preserving useful structural information.

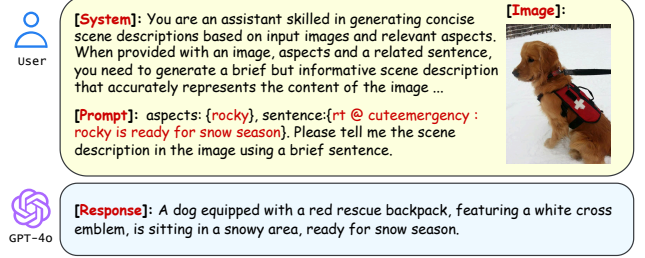


Figure 2: System instructions and prompts for scene graph generation using GPT-4o.

## 3 METHODOLOGY

### 3.1 Preliminaries

**3.1.1 Task Formulation.** Formally, we define three subtasks within MABSA: MATE, MASC, and JMASA. Given a dataset containing multiple samples, each sample consists of an image  $I$  and a sentence  $S$  composed of  $n$  words. The output objectives for these three subtasks are defined as follows:

- JMASA: output =  $[(a_1^b, a_1^e, p_1), \dots, (a_i^b, a_i^e, p_i), \dots]$ ,
- MATE: output =  $[(a_1^b, a_1^e), \dots, (a_i^b, a_i^e), \dots]$ ,
- MASC: output =  $[(\underline{a_1^b}, a_1^e, p_1), \dots, (\underline{a_i^b}, a_i^e, p_i), \dots]$ ,

where  $a_i^b$ ,  $a_i^e$  and  $p_i$  denote the start index, end index, and sentiment polarity of the  $i$ -th aspect term in the sentence, respectively. The underlined token indicates that it was given during inference.

**3.1.2 Scene Graph dataset preparation.** Inspired by Atlantis [36], we incorporate **scene graph** to enhance aspect-specific image semantic extraction. While we adopt Qformer [15] for visual-textual bridging, the original Qformer structure suffers from spatial positional information loss [39]. To overcome this limitation, we utilize GPT-4o [26] to generate structured textual descriptions of images ("Scene Graphs"). This approach not only improves cross-modal alignment but also preserves spatial semantics through Qformer's language modeling capabilities. We implement this solution using carefully designed system-level instructions and prompts for GPT-4o, as illustrated in Figure 2.

### 3.2 Multi-task Pretraining for Base Model

Building on the insights from AESAL [47], VLP [18], and DQPSA [27], we propose a multi-task pre-training strategy that enhances our base model (Qformer and language model) with three critical capabilities: aspect sensitivity, image-text alignment, and sentiment perception. Our approach incorporates three pre-training tasks: aspect-oriented enhancement (AOE), image-text matching (ITM), and aspect-level sentiment-sensitive cognition (ASSC), as illustrated in Figure 3.

**Aspect-Oriented Enhancement** To improve the base model's aspect sensitivity [45, 47], we designed an AOE task (as shown in Figure 3.A). For each sample, we construct a quadruple  $(T, V, S, A)$  - text, visual, scene graph, and aspect term. We then replace the aspect term  $A$  in both text  $T$  and scene graph  $S$  with a special token "[Mask]", resulting in aspect-free text  $T_N$  and scene graph  $S_N$  (as shown in Eq. 2). We treat the original triplet  $(T, V, S)$  as

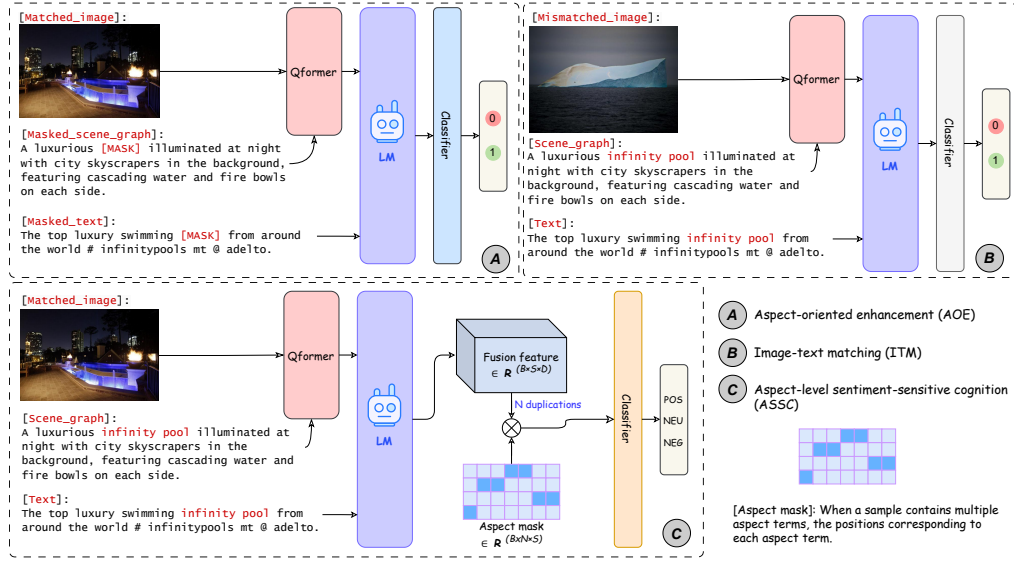


**Figure 3: Multitask pretraining for base model.** We introduce three pre-training tasks—AOE, ITM, and ASSC—to enhance the model’s aspect sensitivity, image-text alignment capability, and sentiment perception ability, respectively. In AOE and ITM tasks, 0 and 1 indicate whether the aspect entities in the image-text pair are aligned and whether the image-text features match. POS, NEU, and NEG represent Positive, Neutral, and Negative.

positive samples  $P_a$  and the masked triplet  $(T_N, V, S_N)$  as negative samples  $N_a$ . This yields a new training set composed of labeled pairs  $[(P_a, L), (N_a, L)]$ , where label  $L = 1$  indicates the presence of aligned aspect terms in the image and text, and  $L = 0$  otherwise. The training objective of AOE is

$$\mathcal{L}_{AOE} = - [L \log(\hat{L}) + (1 - L) \log(1 - \hat{L})]. \quad (1)$$

$$T_N = T.Replace(A, [Mask]), S_N = S.Replace(A, [Mask]). \quad (2)$$

**Image-Text Matching** Following traditional multimodal alignment methods [18, 27], we implemented ITM pretraining for the base model (as shown in Figure 3.B). For each sample containing a triplet  $(T, V, S)$ , we randomly sample an image  $V_N$  different with  $V$  from the dataset, and substitute it into the triplet to form negative samples  $N_b = (T, V_N, S)$ . The original triplet  $(T, V, S)$  serves as positive samples  $P_b$ . This process yields a labeled dataset  $[(P_b, L), (N_b, L)]$ , where  $L = 1$  indicates image-text feature matching, and  $L = 0$  indicates a mismatch. The training objective of ITM is Eq. 3, where  $\hat{L}$  denotes the predicted result.

$$\mathcal{L}_{ITM} = - [L \log(\hat{L}) + (1 - L) \log(1 - \hat{L})]. \quad (3)$$

**Aspect-level Sentiment-Sensitive Cognition** Distinct from existing methods, we propose a novel ASSC task to enhance the model’s sentiment perception ability, thereby addressing the SCP problem (as shown in Figure 3.C). For each sample containing a quintuple  $(T, V, S, A, y_c)$ , where aspect  $A$  contains  $N$  aspect items, we first replicate the language model-generated features  $H \in \mathbb{R}^{B \times S \times D}$   $N$  times, forming a tensor of shape  $\mathbb{R}^{B \times N \times S \times D}$ .  $y_c$  represents sentiment polarity labels. We then apply an aspect mask of shape  $\mathbb{R}^{B \times N \times S}$ , which functions similarly to an attention mask, to guide the model’s focus toward the tokens relevant to each aspect. Finally, through a classifier, we obtain  $N$  sentiment polarity prediction  $\hat{y}_c^{(i)}$

for each aspect. The training objective of ASSC is

$$\mathcal{L}_{ASSC} = - \frac{1}{N} \sum_{i=1}^N \sum_{c=1}^3 y_c^{(i)} \log \hat{y}_c^{(i)}. \quad (4)$$

**Training Objectives** During the pre-training phase, we retain the original loss component  $\mathcal{L}_Q$  from Qformer [15], while incorporating three new pre-training objectives:  $\mathcal{L}_{AOE}$ ,  $\mathcal{L}_{ITM}$ , and  $\mathcal{L}_{ASSC}$ . These four objectives collectively constitute the joint pre-training objective  $\mathcal{L}_p$ , as shown in Eq. 5:

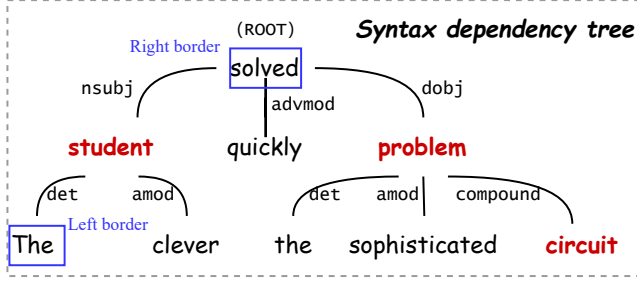
$$\mathcal{L}_p = \mathcal{L}_Q + \mathcal{L}_{AOE} + \mathcal{L}_{ITM} + \mathcal{L}_{ASSC}. \quad (5)$$

### 3.3 Dependency Structure Augmented Contextual Scoping Module

After completing the base model pre-training, we freeze its parameters during subsequent training phase. We propose a dependency structure augmented contextual scoping module (as shown in the Figure 5), which explicitly incorporates dependency relations to improve the model’s syntactic modeling capability by leveraging global syntactic information. This module defines a target-specific scope based on the dependency tree, enabling the model to focus on key semantic features within the scope during classification.

**3.3.1 Target-specific Scope Definition.** To precisely delineate target-related vocabulary, we introduce a target-specific scope based on constituent tree structure that distinguishes between words relevant and irrelevant to the target. Using spaCy<sup>1</sup> for dependency parsing, we obtain syntactic trees. For instance, in “The clever student quickly solved the sophisticated circuit problem,” the dependency tree is illustrated in Figure 4. For a target word, we define

<sup>1</sup>spaCy toolkit: <https://spacy.io/>



[Text]: The clever student quickly solved the sophisticated circuit problem.

[Scope for 'student']: The clever student quickly solved

Figure 4: The definition of target-specific scope.

the scope boundary as the farthest word along its parent-child path in the dependency tree. Taking "student" as an example, its scope encompasses "The clever student quickly solved"—from the leftmost associated word "The" to the rightmost "solved." This method captures important sentiment cues like "quickly" that may not be direct parent-child nodes but remain semantically significant. This approach surpasses traditional dependency-based methods by more comprehensively capturing contextual information semantically related to targets, thereby enhancing effective semantic perception.

**3.3.2 Semantic and Syntactic Graph Construction.** To leverage syntactic structure and semantic information from input sentences, we designed a semantic and syntactic graph construction module.

**Semantic Graph Construction** Following the design in [1], we represent each word in sentence  $S$  as a graph node and employ the self-attention mechanism to calculate similarity scores between word pairs as edge weights, constructing a directed semantic graph (SemGraph). To fully exploit the semantic relationships embedded in SemGraph, we introduce a graph neural network module (SemGNN) to perform feature aggregation on the graph structure, capturing enriched semantic representations  $H^{sem}$ :

$$H_l^{sem} = \text{ReLU}(A^{sem} H_{l-1}^{sem} W_l^{sem} + b_l^{sem}). \quad (6)$$

The adjacency matrix  $A^{sem} \in \mathbb{R}^{S \times S}$  of the SemGraph is defined as follows:

$$A^{sem} = \text{softmax} \left( \frac{(QW_q)(KW_k)^T}{\sqrt{D}} \right), \quad (7)$$

where  $Q$  and  $K$  are two copies of the contextual representation  $H \in \mathbb{R}^{S \times D}$  extracted by the language model (LM), serving as query and key vectors. Learnable parameter matrices  $W_q, W_k \in \mathbb{R}^{D \times D}$  in the self-attention transform the input features linearly.  $D$  represents the dimension of each node feature, and  $S$  is the sentence sequence length. The parameters of the  $l$ -th layer of the SemGNN include the weight matrix  $W_l^{sem} \in \mathbb{R}^{D \times D}$  and the bias term  $b_l^{sem} \in \mathbb{R}^D$ . The initial input  $H_0^{sem}$  of SemGNN is  $H$ , serving as the nodes' initial features.

**Syntactic Graph Construction** For input sentence  $S$ , we first generate its dependency tree  $T$  using spaCy parser. We then construct SynGraph, an undirected graph where each word becomes a graph node and dependency relations from  $T$  form the edges.

To effectively encode syntactic structural information from SynGraph, we implement SynGNN to generate representations  $H^{syn}$  that capture rich global syntactic relationships:

$$H_l^{syn} = \text{ReLU}(A^{syn} H_{l-1}^{syn} W_l^{syn} + b_l^{syn}). \quad (8)$$

The adjacency matrix  $A^{syn} \in \mathbb{R}^{S \times S}$  of the SynGraph is defined as follows:

$$A_{ij}^{syn} = \begin{cases} 1 & \text{if } \text{adj}(i, j) = 1 \text{ or } i = j, \\ 0 & \text{otherwise.} \end{cases}, \quad (9)$$

where  $\text{adj}(i, j)$  indicates the existence of a parent-child dependency relationship between the  $i$ -th word and the  $j$ -th word. The settings of  $W_l^{syn}, b_l^{syn}$ , and  $H_l^{syn}$  are same with those in SemGNN, and SynGNN do not share parameters with SemGNN.

**3.3.3 Adaptive Scope Coupling for Contrastive Graph Learning.** We propose adaptive scope coupling for contrastive graph learning to reduce noise from irrelevant relationships and inflated attention scores in SynGraph and SemGraph. Our method precisely align targets with their opinion words by distinguishing in-scope and out-of-scope words, effectively alleviating the SNE problem. It employs two contrastive strategies: (1) **cross-scope contrast within the same graph**, and (2) **cross-graph contrast between SynGraph and SemGraph for scopes**.

To align target words with their corresponding opinion words and differentiate target-specific scopes, we designed a cross-scope contrastive loss using node representations from SynGraph and SemGraph. Taking SynGraph as an example, let  $\{n_i\}_{i \in [S]}$  represent all node representations and  $Scope_t^n$  the scope for each target. The target node representation  $n_t$  serves as the anchor: any node  $n_j \in Scope_t^n$  forms a *positive* pair with  $n_t$ , while nodes  $n_k \notin Scope_t^n$  are *negative*. Based on the InfoNCE [32] objective, we compute the contrastive loss for all positive pairs  $(n_t, n_j)$  in the sentence as follows:

$$\mathcal{L}_{\text{scope}}^{syn} = -\frac{1}{T} \sum_{t=1}^T \sum_{n_j \in Scope_t^n} \log \frac{\exp(\text{sim}(n_t, n_j)/\tau)}{\sum_{n_i} \exp(\text{sim}(n_t, n_i)/\tau)}, \quad (10)$$

where  $\tau$  is the temperature parameter,  $T$  is the number of target words in the sentence, and  $\text{sim}(\cdot, \cdot)$  denotes cosine similarity. Similarly, we calculate the corresponding scope contrastive loss  $\mathcal{L}_{\text{scope}}^{sem}$  for SemGraph. Finally, the overall **cross-scope** contrastive objective is formally given as:

$$\mathcal{L}_{\text{scope}} = \mathcal{L}_{\text{scope}}^{syn} + \mathcal{L}_{\text{scope}}^{sem}. \quad (11)$$

To further enhance target-specific embeddings and align semantic scopes across graphs, we employ cross-graph contrastive learning integrating heterogeneous graph correlations into our modeling paradigm. This approach applies contrastive learning on corresponding node representations across graphs. Using SynGraph as an example, we designate target node representation  $n_t$  as the anchor. Its counterpart in SemGraph  $m_t$ , along with all nodes within the target-specific scope  $Scope_t^m$  in SemGraph, form the *positive* set, while all other SemGraph nodes are treated as *negative* samples. To emphasize differences among positive samples and boost representational diversity, We introduce a similarity weight  $\omega$  between graphs. The cross-graph contrastive loss for SynGraph is defined

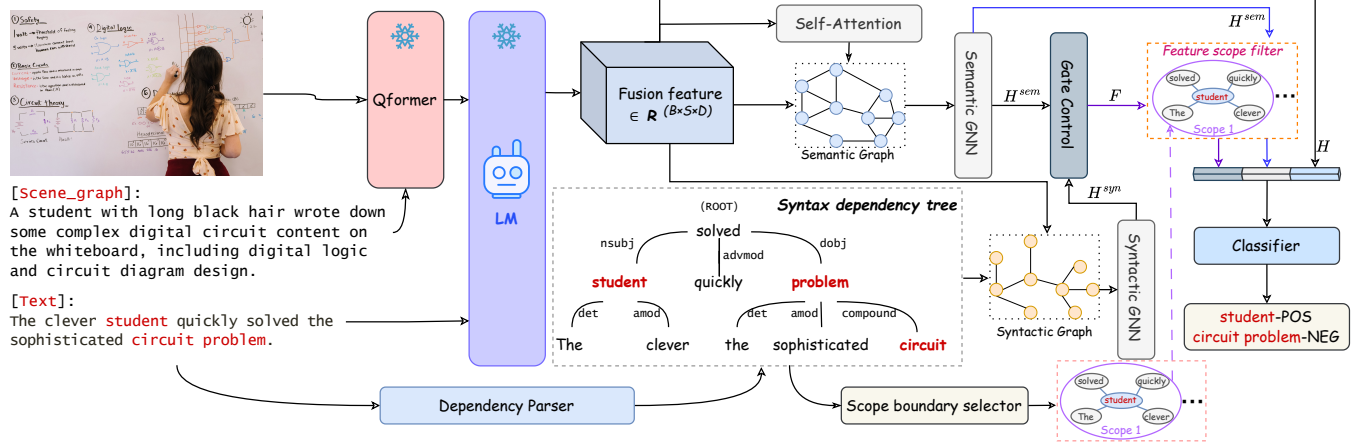


Figure 5: The pipeline of DASCO.

as follows:

$$\mathcal{L}_{m_j} = -\log \frac{\exp(\omega/\tau) + \exp(\omega \cdot \text{sim}(n_t, m_j)/\tau)}{\sum_{m_i} \exp(\text{sim}(n_t, m_i)/\tau)}, \quad (12)$$

$$\mathcal{L}_{\text{graph}}^{\text{syn}} = \frac{1}{T} \sum_{t=1}^T \sum_{m_j \in \text{Scope}_t^n} \mathcal{L}_{m_j}, \quad (13)$$

where  $\omega = \text{sim}(n_t, m_t)$ . Similarly, we calculate the cross-graph contrastive loss  $\mathcal{L}_{\text{graph}}^{\text{sem}}$  for SemGraph. The overall **cross-graph** contrastive objective can be defined as:

$$\mathcal{L}_{\text{graph}} = \mathcal{L}_{\text{graph}}^{\text{syn}} + \mathcal{L}_{\text{graph}}^{\text{sem}}. \quad (14)$$

Eventually, by integrating the cross-scope and cross-graph contrastive components, we formulate the complete loss of the adaptive scope coupling for contrastive graph learning:

$$\mathcal{L}_{\text{cgl}} = \mathcal{L}_{\text{scope}} + \mathcal{L}_{\text{graph}}. \quad (15)$$

**3.3.4 Model Inference and Training.** For **inference**, semantic and syntactic features ( $H^{\text{sem}}$  and  $H^{\text{syn}}$ ) are fused via a gated control mechanism to obtain  $F$ . A scope filter, implemented by a scope mask  $\in \mathbb{R}^{B \times N \times S}$  (similar to an attention mask), performs weighted filtering on  $F$  and  $H^{\text{sem}}$  for each of the  $N$  scopes individually, preserving information within relevant scopes. The filtered representations are then concatenated with  $H$  and passed to the classifier for final prediction.

For **training**, we employ task-specific training strategies tailored to each MABSA sub-tasks. For the MATE task, we extract nouns and pronouns as candidate aspect terms using spaCy and define corresponding scopes for each candidate. Then, a binary classifier is used to determine whether each candidate represents a genuine aspect. The overall training objective is defined as:

$$\mathcal{L}_{\text{MATE}} = -\frac{1}{N} \sum_{i=1}^N [y_i \log \hat{y}_i + (1 - y_i) \log(1 - \hat{y}_i)] + \lambda \cdot \mathcal{L}_{\text{cgl}}, \quad (16)$$

where  $y_i \in \{0, 1\}$  indicates whether a candidate aspect term is genuine,  $\hat{y}_i \in \{0, 1\}$  is the predicted result,  $N$  is the total number of candidate aspect terms, and  $\lambda$  is a hyperparameter.

For the MASC task, each detected aspect term is assigned a contextual scope, within which a three-way classifier predicts its sentiment polarity. The overall training objective is defined as:

$$\mathcal{L}_{\text{MASC}} = -\frac{1}{M} \sum_{j=1}^M \sum_{c=1}^3 y_c^j \log \hat{y}_c^j + \lambda \cdot \mathcal{L}_{\text{cgl}}, \quad (17)$$

where  $y_c^j \in \{0, 1, 2\}$  indicates the sentiment label of aspect term,  $\hat{y}_c^j \in \{0, 1, 2\}$  is the predicted sentiment polarity, and  $M$  is the total number of aspect terms.

For the JMASA task, we sequentially connect the trained MATE and MASC models and perform inference without any additional training.

## 4 EXPERIMENTS

### 4.1 Settings

**Datasets and Metrics** Following previous works, we use Twitter2015 and Twitter2017 as benchmark datasets and build a new Scene Graph dataset based on them (see Section 3.1.2). During pre-training, we generated pre-training data from these Twitter datasets (details in supplementary materials). For evaluation metrics, we report precision (P), recall (R), and Micro-F1 (F1) for MATE and JMASA tasks, and accuracy (Acc) and Macro-F1 (F1) for MASC.

**Implementation Details** DASCO uses Qformer[15] and FUSIE-base [28] as base model, with parameters initialized from the DQPSA [27] model. During pre-training, we set the learning rate to  $5e-5$ , batch size to 4, and train for 50 epochs. In the second phase, we fixed the base model parameters and used a learning rate of  $2e-5$  with a batch size of 16 for 20 epochs, setting the hyperparameter  $\lambda$  to 0.2. The number of layers  $l$  for both SemGNN and SynGNN is 4. All experiments were conducted via distributed training across 8 NVIDIA GeForce RTX 4090 GPUs. The code and checkpoints will be released following publication of this paper.

### 4.2 Main results

We report the main results of our proposed DASCO and various baselines on the JMASA, MATE, and MASC tasks in Tables.

1,2,3. The **bolded** values indicate the best performance, while the underlined values are the second best. Several key observations emerge from these comparisons:

**Table 1: Performance comparison on JMASA task.**

Method	Publication	Twitter2015			Twitter2017		
		P	R	F1	P	R	F1
<i>Text-only</i>							
SPAN[9]	ACL2020	53.7	53.9	53.8	59.6	61.7	60.6
D-GCN[2]	COLING2020	58.3	58.8	59.4	64.1	64.2	64.1
BART[37]	ACL2021	62.9	65.0	63.9	65.2	65.6	65.4
<i>Multimodal</i>							
JML[13]	EMNLP2021	65.0	63.2	64.1	66.5	65.5	66.0
VLP[18]	ACL2022	65.1	68.3	66.6	66.9	69.2	68.2
CMMT[38]	IPM2022	64.6	68.7	66.5	67.6	69.4	68.5
M2DF[44]	EMNLP2023	67.0	67.3	67.6	67.9	68.8	68.3
AoM[46]	ACL2023	67.9	69.3	68.6	68.4	71.0	69.7
MOCOLNET[25]	TKDE2023	66.3	67.9	67.1	67.3	68.7	68.0
DQPSA[27]	AAAI2024	71.7	<u>72.0</u>	<u>71.9</u>	<u>71.1</u>	70.2	70.6
Atlantis[36]	Inf.Fusion2024	65.6	69.2	67.3	68.6	70.3	69.4
ADAR[3]	ACM MM2024	70.0	71.5	71.2	<b>71.6</b>	71.0	<u>71.4</u>
AESAL[47]	IJCAI2024	68.7	70.4	69.5	69.4	<b>74.8</b>	<b>72.0</b>
RNG[23]	ICME2024	67.8	69.5	68.6	69.5	71.0	70.2
Vanessa[35]	EMNLP2024	68.6	71.1	69.8	69.2	72.1	70.6
CORSA[21]	COLING2025	69.0	70.8	69.9	70.1	71.0	70.6
<b>DASCO (Ours)</b>	-	<b>72.7</b>	<b>77.4</b>	<b>75.0</b>	70.6	<u>73.3</u>	<b>72.0</b>

**Results for JMASA** DASCO significantly outperforms all text-only baselines, demonstrating the effectiveness of integrating visual information as complementary cues to textual representations. On Twitter2015, DASCO exceeds the second-best model DQPSA by 3.1 percentage points in F1 score, primarily attribute to our MABSA-specific pretraining strategy enhancing the model’s aspect sensitivity and sentiment perception. On Twitter2017, DASCO maintains the highest F1 score despite slightly lower precision and recall than ADAR and AESAL. DASCO’s performance stems from three key components: (i) a multitask pretraining base model incorporating aspect-oriented enhancement, image-text matching, and aspect-level sentiment-sensitive cognition; (ii) explicit integration of dependency structure maximizing global syntactic information utilization; and (iii) a target-specific scoping mechanism effectively suppresses semantic noise from irrelevant regions.

**Results for MATE and MASC** Tables 2 and 3 report DASCO’s performance on MATE and MASC tasks. Consistent with JMASA results, DASCO achieves state-of-the-art performance across most metrics for both tasks. The sole exception occurs on the MATE task with Twitter2015, where our model shows marginally lower precision than DQPSA and ADAR, while still maintaining the highest F1 score. These findings further validate our approach’s robustness.

### 4.3 Ablation Study

In this section, we compare DASCO’s variants across five components to demonstrate its effectiveness, as shown in Table 4:

**Effect of Scene graph** **W/o Scene graph** replaces structured scene graphs with raw text input to Qformer. This modification results in significant performance decline for JMASA and MATE tasks (except for Recall in MATE), while MASC task performance

**Table 2: Performance comparison on MATE task.**

Method	Publication	Twitter2015			Twitter2017		
		P	R	F1	P	R	F1
RAN[33]	NLPCC2020	80.5	81.5	81.0	90.7	90.7	90.0
UMT[43]	ACL2020	77.8	81.7	79.7	86.7	86.8	86.7
OSCGA[34]	ACM MM2020	81.7	82.1	81.9	90.2	90.7	90.4
JML[13]	EMNLP2021	83.6	81.2	82.4	92.0	90.7	91.4
VLP[18]	ACL2022	83.6	87.9	85.7	90.8	92.6	91.7
CMMT[38]	IPM2022	83.9	<u>88.1</u>	85.9	92.2	<u>93.9</u>	93.1
MNER-QG[12]	AAAI2023	77.4	72.1	74.7	88.2	85.6	86.9
Prompt-Me-Up[10]	ACM MM2023	80.0	80.9	80.5	91.7	91.3	91.6
M2DF[44]	EMNLP2023	85.0	87.2	86.1	91.2	93.0	92.2
AoM[46]	ACL2023	84.6	87.9	86.2	91.8	92.8	92.3
MOCOLNET[25]	TKDE2023	85.3	87.0	86.1	91.5	92.9	91.7
DQPSA[27]	AAAI2024	<b>88.3</b>	87.1	<u>87.7</u>	<u>95.1</u>	93.5	<u>94.3</u>
Atlantis[36]	Inf.Fusion2024	84.2	87.7	86.1	91.8	93.2	92.7
ADAR[3]	ACM MM2024	<u>86.5</u>	88.0	87.2	93.0	<u>93.9</u>	93.4
CORSA[21]	COLING2025	85.1	87.6	86.3	92.6	93.0	92.8
<b>DASCO (Ours)</b>	-	86.4	<b>92.3</b>	<b>89.2</b>	<b>95.6</b>	<b>96.1</b>	<b>95.8</b>

**Table 3: Performance comparison on MASC task.**

Method	Publication	Twitter2015		Twitter2017	
		ACC	F1	ACC	F1
ESAFN[42]	TASLP2019	73.4	67.4	67.8	64.2
TomBERT[41]	IJCAI2019	77.2	71.8	70.5	68.0
CapTrBERT[14]	ACM MM2020	78.0	73.2	72.3	70.2
JML[13]	EMNLP2021	76.1	72.3	72.3	69.9
VLP[18]	ACL2022	78.6	73.8	73.8	71.8
CMMT[38]	IPM2022	77.9	-	73.8	-
M2DF[44]	EMNLP2023	78.9	74.8	74.3	73.0
AoM[46]	ACL2023	80.2	75.9	76.4	75.0
DQPSA[27]	AAAI2024	81.1	-	75.0	-
Atlantis[36]	Inf.Fusion2024	79.3	-	74.2	-
ADAR[3]	ACM MM2024	<u>81.3</u>	77.1	77.2	<u>76.6</u>
AESAL[47]	IJCAI2024	80.1	75.2	<u>78.8</u>	75.9
CORSA[21]	COLING2025	81.1	<u>77.7</u>	76.6	74.5
<b>DASCO (Ours)</b>	-	<b>83.8</b>	<b>78.8</b>	<b>79.5</b>	<b>76.9</b>

remains relatively stable, even showing slight ACC improvement on Twitter2015. These findings suggest that structured image descriptions enhance Qformer’s textual-visual integration capability, improving aspect entity comprehension.

**Effect of Scope** **W/o Scope** substitutes the original scope with only the target word’s position, substantially degrading performance. This validates our scope construction strategy’s effectiveness in modeling semantic boundaries.

**Effect of Syntactic branch** **W/o Syntactic** removes the dependency parse tree-based syntactic branch, retaining only the original representation  $H$  and semantic branch representation  $H^{sem}$ . The notable performance decline demonstrates syntactic information’s crucial role in mitigating noise interference and extracting relevant features.

**Effect of Semantic branch** **W/o Semantic** eliminates the semantic branch while maintaining the original representation  $H$

**Table 4: The performance comparison of our full model and its ablated methods on JMASA, MATE and MASC.**

Variants	JMASA						MATE						MASC			
	Twitter2015			Twitter2017			Twitter2015			Twitter2017			Twitter2015		Twitter2017	
	P	R	F1	ACC	F1	ACC	F1									
Full	<b>72.7</b>	<b>77.4</b>	<b>75.0</b>	<b>70.6</b>	<b>73.3</b>	<b>72.0</b>	<b>86.4</b>	92.3	<b>89.2</b>	<b>95.6</b>	96.1	<b>95.8</b>	83.8	<b>78.8</b>	<b>79.5</b>	<b>76.9</b>
w/o Scene graph	68.1	77.1	72.3	67.9	72.4	70.1	81.5	<b>92.4</b>	86.6	91.1	97.1	94.0	<b>83.9</b>	78.3	78.8	76.3
w/o Scope	66.9	75.5	70.9	66.1	72.3	69.1	81.4	92.1	86.4	89.0	97.2	93.0	82.7	77.2	72.1	70.8
w/o Syntactic	54.9	61.8	58.1	61.7	68.7	65.0	67.9	71.5	69.7	76.0	86.3	80.8	75.1	71.2	68.3	65.2
w/o Semantic	69.1	76.3	72.5	61.8	67.0	64.3	86.2	91.2	86.7	90.1	<b>97.6</b>	93.7	82.2	77.4	75.1	73.3
w/o Pretraining	58.4	63.7	61.0	60.8	64.3	62.5	84.6	91.6	88.0	92.0	96.7	94.3	75.5	72.1	67.3	64.6

and syntactic branch representation  $H^{syn}$ . This configuration experiences moderate performance decrease, indicating  $H^{syn}$ 's robust sentiment expression capabilities and confirming the syntactic branch's advantages in aspect relevance and sentiment perception. **Effect of Multi-task pretraining** **W/o Pretraining** omits multi-task pretraining, directly unfreezing and training the base model. Results reveal limited performance variation in the MATE task but significant deterioration in the MASC, substantiating our multi-task pretraining strategy's effectiveness in enhancing sentiment cognition capabilities and alleviating the SCP problem.

**Table 5: Comparison with LLMs on MASC task.**

Models	Twitter2015		Twitter2017	
	ACC	F1	ACC	F1
VisualGLM-6B	66.7	67.2	68.1	67.9
GPT3.5	65.3	66.6	67.0	67.1
GPT4V	75.6	74.3	75.5	75.2
<b>DASCO (ours)</b>	<b>83.8</b>	<b>78.8</b>	<b>79.5</b>	<b>76.9</b>

#### 4.4 Comparison with LLMs on MASC

To validate DASCO's competitiveness in MABSA, we compared it with mainstream LLMs including VisualGLM-6B, GPT-3.5, and GPT-4V. Given LLMs' inherent limitations in aspect identification and structured output, comparisons were restricted to the MASC task for evaluation fairness. We defined roles and system instructions for each LLM and provided image, text, and aspect information as input (GPT-3.5 received only text and aspect inputs due to its unimodal nature). Results in Table 5 demonstrate that despite DASCO's parameter significantly smaller parameter scale compared to LLMs, it exhibits superior performance, confirming its effectiveness in multimodal sentiment understanding tasks.

#### 4.5 Computation Efficiency

Furthermore, we analyzed the computational efficiency of DASCO compared to several classical models under consistent settings. As shown in Table 6, DASCO demonstrates superior inference speed on the Twitter2015/2017 test sets. During inference, DASCO avoids complex attention mechanisms [13, 46], eliminates calculations of

numerous atomic feature similarities [46], and differs from autoregressive decoding architectures like BART [18]. Instead, it employs only two concise GNN modules, significantly enhancing inference efficiency while maintaining performance.

**Table 6: Comparison on computation efficiency.**

Methods	Twitter2015	Twitter2017
JML[13]	22.390s	17.507s
VLP[18]	29.297s	18.165s
AoM[46]	30.609s	46.481s
DQPSA[27]	80.943s	93.177s
<b>DASCO(ours)</b>	<b>14.248s</b>	<b>11.108s</b>

## 5 CONCLUSION

This paper proposes a Dependency Structure Augmented Contextual Scoping Framework (DASCO) that effectively addresses multimodal information misalignment and sentiment cue perception challenges through multi-task base model pretraining. The introduced dependency structure and target-specific scope strategy further help the model filter irrelevant noise, enhancing semantic interference suppression. Extensive experiments on two benchmark datasets demonstrate the superiority of our method, with significant improvements in JMASA task (Notably achieving +3.1% F1 score and +5.4% precision on Twitter2015) and 37% faster inference than the current fastest approach on both two datasets.

## 6 LIMITATIONS AND INSIGHTS

Despite achieving state-of-the-art performance, our model exhibits limitations in processing efficiency, as sentiment classification and aspect extraction require individual target word analysis, limiting parallelism. Nonetheless, experimental results confirm that multi-task pretraining significantly enhances sentiment cue perception and image-text alignment capabilities, effectively addressing the SCP and MIM challenges. Additionally, the explicitly integrated dependency structure provides global syntactic information which, combined with the target-specific scope strategy, produces effective semantic noise elimination (SNE). Future research should focus on these three critical challenges—SCP, MIM, and SNE—to advance MABSA task development.

## REFERENCES

- [1] Heyan Chai, Ziyi Yao, Siyu Tang, Ye Wang, Liqiang Nie, Binxing Fang, and Qing Liao. 2023. Aspect-to-Scope Oriented Multi-view Contrastive Learning for Aspect-based Sentiment Analysis. In *Findings of the Association for Computational Linguistics: EMNLP 2023, Singapore, December 6-10, 2023*. Association for Computational Linguistics, 10902–10913. <https://doi.org/10.18653/V1/2023.FINDINGS-EMNLP.727>
- [2] Guimin Chen, Yuanhe Tian, and Yan Song. 2020. Joint Aspect Extraction and Sentiment Analysis with Directional Graph Convolutional Networks. In *Proceedings of the 28th International Conference on Computational Linguistics, COLING 2020, Barcelona, Spain (Online), December 8-13, 2020*. International Committee on Computational Linguistics, 272–279. <https://doi.org/10.18653/V1/2020.COLING-MAIN.24>
- [3] Zhanpeng Chen, Zhihong Zhu, Wanshi Xu, Yunyan Zhang, Xian Wu, and Yefeng Zheng. 2024. *Aspects are Anchors: Towards Multimodal Aspect-based Sentiment Analysis via Aspect-driven Alignment and Refinement*. In *Proceedings of the 32nd ACM International Conference on Multimedia, MM 2024, Melbourne, VIC, Australia, 28 October 2024 - 1 November 2024*. ACM, 2292–2300. <https://doi.org/10.1145/3664647.3681189>
- [4] Junqi Dai, Hang Yan, Tianxiang Sun, Pengfei Liu, and Xipeng Qiu. 2021. Does syntax matter? A strong baseline for Aspect-based Sentiment Analysis with RoBERTa. In *Proceedings of the 2021 Conference of the North American Chapter of the Association for Computational Linguistics: Human Language Technologies, NAACL-HLT 2021, Online, June 6-11, 2021*. Association for Computational Linguistics, 1816–1829. <https://doi.org/10.18653/V1/2021.NAACL-MAIN.146>
- [5] Jacob Devlin, Ming-Wei Chang, Kenton Lee, and Kristina Toutanova. 2019. BERT: Pre-training of Deep Bidirectional Transformers for Language Understanding. In *Proceedings of the 2019 Conference of the North American Chapter of the Association for Computational Linguistics: Human Language Technologies, NAACL-HLT 2019, Minneapolis, MN, USA, June 2-7, 2019, Volume 1 (Long and Short Papers)*. Association for Computational Linguistics, 4171–4186. <https://doi.org/10.18653/V1/N19-1423>
- [6] Alexey Dosovitskiy, Lucas Beyer, Alexander Kolesnikov, Dirk Weissenborn, Xi-aohua Zhai, Thomas Unterthiner, Mostafa Dehghani, Matthias Minderer, Georg Heigold, Sylvain Gelly, Jakob Uszkoreit, and Neil Houlsby. 2021. An Image is Worth 16x16 Words: Transformers for Image Recognition at Scale. In *9th International Conference on Learning Representations, ICLR 2021, Virtual Event, Austria, May 3-7, 2021*. OpenReview.net. <https://openreview.net/forum?id=YicbFdNTTy>
- [7] Junjia Feng, Mingqian Lin, Lin Shang, and Xiaoying Gao. 2024. Autonomous Aspect-Image Instruction a2II: Q-Former Guided Multimodal Sentiment Classification. In *Proceedings of the 2024 Joint International Conference on Computational Linguistics, Language Resources and Evaluation, LREC/COLING 2024, 20-25 May, 2024, Torino, Italy*. ELRA and ICCL, 1996–2005. <https://aclanthology.org/2024.lrec-main.180>
- [8] Lijun He, Zhihan Ren, Wanyue Zhang, Fan Li, and Shaohui Mei. 2024. Unsupervised Pansharpening Based on Double-Cycle Consistency. *IEEE Transactions on Geoscience and Remote Sensing* (2024).
- [9] Minghao Hu, Yuxing Peng, Zhen Huang, Dongsheng Li, and Yiwei Lv. 2019. Open-Domain Targeted Sentiment Analysis via Span-Based Extraction and Classification. In *Proceedings of the 57th Conference of the Association for Computational Linguistics, ACL 2019, Florence, Italy, July 28- August 2, 2019, Volume 1: Long Papers*. Association for Computational Linguistics, 537–546. <https://doi.org/10.18653/V1/P19-1051>
- [10] Xuming Hu, Junzhe Chen, Aiwei Liu, Shiao Meng, Lijie Wen, and Philip S. Yu. 2023. Prompt Me Up: Unleashing the Power of Alignments for Multimodal Entity and Relation Extraction. In *Proceedings of the 31st ACM International Conference on Multimedia, MM 2023, Ottawa, ON, Canada, 29 October 2023- 3 November 2023*. ACM, 5185–5194. <https://doi.org/10.1145/3581783.3611899>
- [11] Shizhou Huang, Bo Xu, Changqun Li, Jiabo Ye, and Xin Lin. 2024. MNER-MI: A Multi-image Dataset for Multimodal Named Entity Recognition in Social Media. In *Proceedings of the 2024 Joint International Conference on Computational Linguistics, Language Resources and Evaluation, LREC/COLING 2024, 20-25 May, 2024, Torino, Italy*. ELRA and ICCL, 11452–11462. <https://aclanthology.org/2024.lrec-main.1001>
- [12] Meihuizi Jia, Lei Shen, Xin Shen, Lejian Liao, Meng Chen, Xiaodong He, Zhendong Chen, and Jiaqi Li. 2023. MNER-QG: An End-to-End MRC Framework for Multimodal Named Entity Recognition with Query Grounding. In *Thirty-Seventh AAAI Conference on Artificial Intelligence, AAAI 2023, Thirty-Fifth Conference on Innovative Applications of Artificial Intelligence, IAAI 2023, Thirteenth Symposium on Educational Advances in Artificial Intelligence, EAAI 2023, Washington, DC, USA, February 7-14, 2023*. AAAI Press, 8032–8040. <https://doi.org/10.1609/AAAI.V37I7.25971>
- [13] Xincheng Ju, Dong Zhang, Rong Xiao, Junhui Li, Shoushan Li, Min Zhang, and Guodong Zhou. 2021. Joint Multi-modal Aspect-Sentiment Analysis with Auxiliary Cross modal Relation Detection. In *Proceedings of the 2021 Conference on Empirical Methods in Natural Language Processing, EMNLP 2021, Virtual Event / Punta Cana, Dominican Republic, 7-11 November, 2021*. Association for Computational Linguistics, 4395–4405. <https://doi.org/10.18653/V1/2021.EMNLP-MAIN.360>
- [14] Zaid Khan and Yun Fu. 2021. Exploiting BERT for Multimodal Target Sentiment Classification through Input Space Translation. In *MM '21: ACM Multimedia Conference, Virtual Event, China, October 20 - 24, 2021*. ACM, 3034–3042. <https://doi.org/10.1145/3474085.3475692>
- [15] Junnan Li, Dongxu Li, Silvio Savarese, and Steven C. H. Hoi. 2023. BLIP-2: Bootstrapping Language-Image Pre-training with Frozen Image Encoders and Large Language Models. In *International Conference on Machine Learning, ICML 2023, 23-29 July 2023, Honolulu, Hawaii, USA (Proceedings of Machine Learning Research, Vol. 202)*. PMLR, 19730–19742. <https://proceedings.mlr.press/v202/li23q.html>
- [16] Jinyuan Li, Han Li, Di Sun, Jiahao Wang, Wenkun Zhang, Zan Wang, and Gang Pan. 2024. LLMs as Bridges: Reformulating Grounded Multimodal Named Entity Recognition. In *Findings of the Association for Computational Linguistics, ACL 2024, Bangkok, Thailand and virtual meeting, August 11-16, 2024*. Association for Computational Linguistics, 1302–1318. <https://doi.org/10.18653/V1/2024.FINDINGS-ACL.76>
- [17] Ziyang Li, Jianfei Yu, Jia Yang, Wenya Wang, Li Yang, and Rui Xia. 2024. Generative Multimodal Data Augmentation for Low-Resource Multimodal Named Entity Recognition. In *Proceedings of the 32nd ACM International Conference on Multimedia, MM 2024, Melbourne, VIC, Australia, 28 October 2024 - 1 November 2024*. ACM, 7336–7345. <https://doi.org/10.1145/3664647.3681598>
- [18] Yan Ling, Jianfei Yu, and Rui Xia. 2022. Vision-Language Pre-Training for Multimodal Aspect-Based Sentiment Analysis. In *Proceedings of the 60th Annual Meeting of the Association for Computational Linguistics (Volume 1: Long Papers), ACL 2022, Dublin, Ireland, May 22-27, 2022*. Association for Computational Linguistics, 2149–2159. <https://doi.org/10.18653/V1/2022.ACL-LONG.152>
- [19] Hao Liu, Lijun He, and Jiayi Liang. 2024. Joint Modal Circular Complementary Attention for Multimodal Aspect-Based Sentiment Analysis. In *IEEE International Conference on Multimedia and Expo, ICME 2024 - Workshops, Niagara Falls, ON, Canada, July 15-19, 2024*. IEEE, 1–6. <https://doi.org/10.1109/ICMEW63481.2024.10645483>
- [20] Hao Liu, Lijun He, Miao Zhang, and Fan Li. 2024. VADiffusion: Compressed Domain Information Guided Conditional Diffusion for Video Anomaly Detection. *IEEE Trans. Circuits Syst. Video Technol.* 34, 9 (2024), 8398–8411. <https://doi.org/10.1109/TCSVT.2024.3382633>
- [21] Xinjing Liu, Ruifan Li, Shuqin Ye, Guangwei Zhang, and Xiaojie Wang. 2025. Multimodal Aspect-Based Sentiment Analysis under Conditional Relation. In *Proceedings of the 31st International Conference on Computational Linguistics, COLING 2025, Abu Dhabi, UAE, January 19-24, 2025*. Association for Computational Linguistics, 313–323. <https://aclanthology.org/2025.coling-main.22/>
- [22] Yinhan Liu, Myle Ott, Naman Goyal, Jingfei Du, Mandar Joshi, Danqi Chen, Omer Levy, Mike Lewis, Luke Zettlemoyer, and Veselin Stoyanov. 2019. RoBERTa: A Robustly Optimized BERT Pretraining Approach. *CoRR abs/1907.11692* (2019). arXiv:1907.11692 <http://arxiv.org/abs/1907.11692>
- [23] Yaxin Liu, Yan Zhou, Ziming Li, Jinchuan Zhang, Yu Shang, Chenyang Zhang, and Songlin Hu. 2024. RNG: Reducing Multi-level Noise and Multi-grained Semantic Gap for Joint Multimodal Aspect-Sentiment Analysis. In *IEEE International Conference on Multimedia and Expo, ICME 2024, Niagara Falls, ON, Canada, July 15-19, 2024*. IEEE, 1–6. <https://doi.org/10.1109/ICME57554.2024.10687372>
- [24] Fukun Ma, Xuming Hu, Aiwei Liu, Yawen Yang, Shuang Li, Philip S. Yu, and Lijie Wen. 2023. AMR-based Network for Aspect-based Sentiment Analysis. In *Proceedings of the 61st Annual Meeting of the Association for Computational Linguistics (Volume 1: Long Papers), ACL 2023, Toronto, Canada, July 9-14, 2023*. Association for Computational Linguistics, 322–337. <https://doi.org/10.18653/V1/2023.ACL-LONG.19>
- [25] Jie Mu, Feiping Nie, Wei Wang, Jian Xu, Jing Zhang, and Han Liu. 2024. MOCOL-Net: A Momentum Contrastive Learning Network for Multimodal Aspect-Level Sentiment Analysis. *IEEE Trans. Knowl. Data Eng.* 36, 12 (2024), 8787–8800. <https://doi.org/10.1109/TKDE.2023.3345022>
- [26] OpenAI. 2023. GPT-4 Technical Report. *CoRR abs/2303.08774* (2023). <https://doi.org/10.48550/ARXIV.2303.08774> arXiv:2303.08774
- [27] Tianshuo Peng, Zuchao Li, Ping Wang, Lefei Zhang, and Hai Zhao. 2024. A Novel Energy Based Model Mechanism for Multi-Modal Aspect-Based Sentiment Analysis. In *Thirty-Eighth AAAI Conference on Artificial Intelligence, AAAI 2024, Thirty-Sixth Conference on Innovative Applications of Artificial Intelligence, IAAI 2024, Fourteenth Symposium on Educational Advances in Artificial Intelligence, EAAI 2024, February 20-27, 2024, Vancouver, Canada*. AAAI Press, 18869–18878. <https://doi.org/10.1609/AAAI.V38I17.29852>
- [28] Tianshuo Peng, Zuchao Li, Lefei Zhang, Bo Du, and Hai Zhao. 2023. FSUIE: A Novel Fuzzy Span Mechanism for Universal Information Extraction. In *Proceedings of the 61st Annual Meeting of the Association for Computational Linguistics (Volume 1: Long Papers), ACL 2023, Toronto, Canada, July 9-14, 2023*. Association for Computational Linguistics, 16318–16333. <https://doi.org/10.18653/V1/2023.ACL-LONG.902>
- [29] Alec Radford, Jong Wook Kim, Chris Hallacy, Aditya Ramesh, Gabriel Goh, Sandhini Agarwal, Girish Sastry, Amanda Askell, Pamela Mishkin, Jack Clark, Gretchen Krueger, and Ilya Sutskever. 2021. Learning Transferable Visual

- Models From Natural Language Supervision. In *Proceedings of the 38th International Conference on Machine Learning, ICML 2021, 18-24 July 2021, Virtual Event (Proceedings of Machine Learning Research, Vol. 139)*. PMLR, 8748–8763. <http://proceedings.mlr.press/v139/radford21a.html>
- [30] Zhihan Ren, Lijun He, and Jichuan Lu. 2023. Context Aware Edge-Enhanced GAN for Remote Sensing Image Super-Resolution. *IEEE Journal of Selected Topics in Applied Earth Observations and Remote Sensing* (2023).
- [31] Hao Tang, Donghong Ji, Chenliang Li, and Qiji Zhou. 2020. Dependency Graph Enhanced Dual-transformer Structure for Aspect-based Sentiment Classification. In *Proceedings of the 58th Annual Meeting of the Association for Computational Linguistics, ACL 2020, Online, July 5-10, 2020*. Association for Computational Linguistics, 6578–6588. <https://doi.org/10.18653/V1/2020.ACL-MAIN.588>
- [32] Aaron van den Oord, Yazhe Li, and Oriol Vinyals. 2018. Representation Learning with Contrastive Predictive Coding. *CoRR* abs/1807.03748 (2018). [arXiv:1807.03748](http://arxiv.org/abs/1807.03748) <http://arxiv.org/abs/1807.03748>
- [33] Hanqian Wu, Siliang Cheng, Jingjing Wang, Shoushan Li, and Lian Chi. 2020. Multimodal Aspect Extraction with Region-Aware Alignment Network. In *Natural Language Processing and Chinese Computing - 9th CCF International Conference, NLPCC 2020, Zhengzhou, China, October 14-18, 2020, Proceedings, Part I*, Vol. 12430. Springer, 145–156. [https://doi.org/10.1007/978-3-030-60450-9\\_12](https://doi.org/10.1007/978-3-030-60450-9_12)
- [34] Zhiwei Wu, Changmeng Zheng, Yi Cai, Junying Chen, Ho-fung Leung, and Qing Li. 2020. Multimodal Representation with Embedded Visual Guiding Objects for Named Entity Recognition in Social Media Posts. In *MM '20: The 28th ACM International Conference on Multimedia, Virtual Event / Seattle, WA, USA, October 12-16, 2020*. ACM, 1038–1046. <https://doi.org/10.1145/3394171.3413650>
- [35] Luwei Xiao, Rui Mao, Xulang Zhang, Liang He, and Erik Cambria. 2024. Vanessa: Visual Connotation and Aesthetic Attributes Understanding Network for Multimodal Aspect-based Sentiment Analysis. In *Findings of the Association for Computational Linguistics: EMNLP 2024, Miami, Florida, USA, November 12-16, 2024*. Association for Computational Linguistics, 11486–11500. <https://aclanthology.org/2024.findings-emnlp.671>
- [36] Luwei Xiao, Xingjiao Wu, Junjie Xu, Weijie Li, Cheng Jin, and Liang He. 2024. Atlantis: Aesthetic-oriented multiple granularities fusion network for joint multimodal aspect-based sentiment analysis. *Inf. Fusion* 106 (2024), 102304. <https://doi.org/10.1016/J.INFFUS.2024.102304>
- [37] Hang Yan, Junqi Dai, Tuo Ji, Xipeng Qiu, and Zheng Zhang. 2021. A Unified Generative Framework for Aspect-based Sentiment Analysis. In *Proceedings of the 59th Annual Meeting of the Association for Computational Linguistics and the 11th International Joint Conference on Natural Language Processing, ACL/IJCNLP 2021, (Volume 1: Long Papers), Virtual Event, August 1-6, 2021*. Association for Computational Linguistics, 2416–2429. <https://doi.org/10.18653/V1/2021.ACL-LONG.188>
- [38] Li Yang, Jin-Cheon Na, and Jianfei Yu. 2022. Cross-Modal Multitask Transformer for End-to-End Multimodal Aspect-Based Sentiment Analysis. *Inf. Process. Manag.* 59, 5 (2022), 103038. <https://doi.org/10.1016/J.IJPM.2022.103038>
- [39] Linli Yao, Lei Li, Shuhuai Ren, Lean Wang, Yuanxin Liu, Xu Sun, and Lu Hou. 2024. DeCo: Decoupling Token Compression from Semantic Abstraction in Multimodal Large Language Models. *CoRR* abs/2405.20985 (2024). <https://doi.org/10.48550/ARXIV.2405.20985> [arXiv:2405.20985](http://arxiv.org/abs/2405.20985)
- [40] Jianfei Yu, Kai Chen, and Rui Xia. 2023. Hierarchical Interactive Multimodal Transformer for Aspect-Based Multimodal Sentiment Analysis. *IEEE Trans. Affect. Comput. 14*, 3 (2023), 1966–1978. <https://doi.org/10.1109/TAFFC.2023.3171091>
- [41] Jianfei Yu and Jing Jiang. 2019. Adapting BERT for Target-Oriented Multimodal Sentiment Classification. In *Proceedings of the Twenty-Eighth International Joint Conference on Artificial Intelligence, IJCAI 2019, Macao, China, August 10-16, 2019*. ijcai.org, 5408–5414. <https://doi.org/10.24963/IJCAI.2019/751>
- [42] Jianfei Yu, Jing Jiang, and Rui Xia. 2020. Entity-Sensitive Attention and Fusion Network for Entity-Level Multimodal Sentiment Classification. *IEEE ACM Trans. Audio Speech Lang. Process.* 28 (2020), 429–439. <https://doi.org/10.1109/TASLP.2019.2957872>
- [43] Jianfei Yu, Jing Jiang, Li Yang, and Rui Xia. 2020. Improving Multimodal Named Entity Recognition via Entity Span Detection with Unified Multimodal Transformer. In *Proceedings of the 58th Annual Meeting of the Association for Computational Linguistics, ACL 2020, Online, July 5-10, 2020*. Association for Computational Linguistics, 3342–3352. <https://doi.org/10.18653/V1/2020.ACL-MAIN.306>
- [44] Fei Zhao, Chunhui Li, Zhen Wu, Yawen Ouyang, Jianbing Zhang, and Xinyu Dai. 2023. M2DF: Multi-grained Multi-curriculum Denoising Framework for Multimodal Aspect-based Sentiment Analysis. In *Proceedings of the 2023 Conference on Empirical Methods in Natural Language Processing, EMNLP 2023, Singapore, December 6-10, 2023*. Association for Computational Linguistics, 9057–9070. <https://doi.org/10.18653/V1/2023.EMNLP-MAIN.561>
- [45] Ziwei Zheng, Lijun He, Le Yang, and Fan Li. 2024. Fine-Grained Dynamic Network for Generic Event Boundary Detection. In *European Conference on Computer Vision*. Springer, 107–123.
- [46] Ru Zhou, Wenya Guo, Xumeng Liu, Shenglong Yu, Ying Zhang, and Xiaojie Yuan. 2023. AoM: Detecting Aspect-oriented Information for Multimodal Aspect-Based Sentiment Analysis. In *Findings of the Association for Computational Linguistics: ACL 2023, Toronto, Canada, July 9-14, 2023*. Association for Computational Linguistics, 8184–8196. <https://doi.org/10.18653/V1/2023.FINDINGS-ACL.519>
- [47] Linlin Zhu, Heli Sun, Qunshu Gao, Tingzhou Yi, and Liang He. 2024. Joint Multimodal Aspect Sentiment Analysis with Aspect Enhancement and Syntactic Adaptive Learning. In *Proceedings of the Thirty-Third International Joint Conference on Artificial Intelligence, IJCAI 2024, Jeju, South Korea, August 3-9, 2024*. ijcai.org, 6678–6686. <https://www.ijcai.org/proceedings/2024/738>